

## Article

# Sustainable Groundwater Potential Zoning with Integrating GIS, Remote Sensing, and AHP Model: A Case from North-Central Bangladesh

Ujjayini Priya <sup>1</sup>, Muhammad Anwar Iqbal <sup>1</sup>, Mohammed Abdus Salam <sup>1,\*</sup>, Md. Nur-E-Alam <sup>1</sup>,  
Mohammed Faruque Uddin <sup>2</sup>, Abu Reza Md. Towfiqul Islam <sup>3</sup>, Showmitra Kumar Sarkar <sup>4</sup>,  
Saiful Islam Imran <sup>5</sup> and Aweng Eh Rak <sup>6</sup>

<sup>1</sup> Department of Environmental Science and Disaster Management, Noakhali Science and Technology University, Noakhali 3814, Bangladesh; ujjayinipriya.nstu11@gmail.com (U.P.); anwariqbalesdm@gmail.com (M.A.I.); nalam.nstu54@gmail.com (M.N.-E.-A.)

<sup>2</sup> Department of Sociology, Shahjalal University of Science and Technology, Sylhet 3114, Bangladesh; faruq-soc@sust.edu

<sup>3</sup> Department of Disaster Management, Begum Rokeya University, Rangpur 5400, Bangladesh; towfiq\_dm@brur.ac.bd

<sup>4</sup> Department of Urban and Regional Planning, Khulna University of Engineering and Technology, Khulna 9203, Bangladesh; mail4dhrubo@gmail.com

<sup>5</sup> Department of Environmental Science, Khulna University, Khulna 9208, Bangladesh; saifulimranes@gmail.com

<sup>6</sup> Faculty of Earth Science, University Malaysia Kelantan, Jeli Campus, Jeli 17600, Kelantan, Malaysia; aweng@umk.edu.my

\* Correspondence: s\_salam1978@yahoo.com; Tel.: +88-019-1763-5348



**Citation:** Priya, U.; Iqbal, M.A.; Salam, M.A.; Nur-E-Alam, M.; Uddin, M.F.; Islam, A.R.M.T.; Sarkar, S.K.; Imran, S.I.; Rak, A.E. Sustainable Groundwater Potential Zoning with Integrating GIS, Remote Sensing, and AHP Model: A Case from North-Central Bangladesh. *Sustainability* **2022**, *14*, 5640. <https://doi.org/10.3390/su14095640>

Academic Editors: Andreas N. Angelakis and Hone-Jay Chu

Received: 8 March 2022

Accepted: 5 May 2022

Published: 7 May 2022

**Publisher's Note:** MDPI stays neutral with regard to jurisdictional claims in published maps and institutional affiliations.



**Copyright:** © 2022 by the authors. Licensee MDPI, Basel, Switzerland. This article is an open access article distributed under the terms and conditions of the Creative Commons Attribution (CC BY) license (<https://creativecommons.org/licenses/by/4.0/>).

**Abstract:** Groundwater is one of the most valuable natural resources, and the most dependable source of fresh water. For sustainable groundwater management, the present study aimed to model groundwater potential zones in the north–central region of Bangladesh using GIS, remote sensing, and the analytical hierarchy process. The present study included eight thematic layers: lineament density, geomorphology, soil types, slope, land use/land cover, drainage density, elevation, and rainfall features to delineate a groundwater potential zone of the area. Integration of the eight thematic layers was performed through weighted overlay analysis, which assisted in delineating groundwater potential zones. This simple and systematic method successfully provides a satisfactory result concerning the delineation of groundwater potential zones. The study resulted in a groundwater potential zone map, which identifies about 11.51% of the study area as being under a very high groundwater potential zone, covering an area of 504.09 km<sup>2</sup>. The AHP analysis shows that the physiographical parameters, such as lineament density, slope, and drainage density, and meteorological factors such as annual rainfall, have greater influence over groundwater potentiality. The result obtained from the weighted overlay analysis was verified with actual well yield and groundwater depth data, which show a significant positive correlation. The outcome of the study will help in taking effective measures to ensure sustainable use and extraction of groundwater in this region.

**Keywords:** groundwater potential zone; groundwater sustainability; well yield; AHP; Bangladesh

## 1. Introduction

Nature's greatest gift, water, is essential to human civilization, primarily for drinking, irrigation, industry, and other purposes. Almost three-quarters of the Earth's surface is covered with water, but freshwater resources are limited [1]. Groundwater plays an important role in meeting freshwater demands, particularly for drinking water [2]. As a primary source of clean, potable water in all climatic regions, groundwater is recognized as one of the most valuable natural resources [3]. Therefore, groundwater supplies irrigation

water for one-quarter of the world's irrigated farmland, and 75 percent of these areas are in Asia [4]. Many regions across the world, particularly in rural areas, rely only on wells and springs for their water supply. Population growth, urbanization, and industrialization have all had an effect on the availability of fresh water sources over time [5]. The global aquifer recharge–withdrawal balance is being disturbed due to excessive groundwater withdrawal [6].

Groundwater is the principal source of fresh water in Bangladesh, and demand for groundwater escalated since the 1980s [7]. The agricultural sector of Bangladesh is largely dependent on groundwater, and 79.1% of the agricultural land is irrigated by groundwater [8]. In the last two decades, increased groundwater accessibility helped Bangladesh achieve near self-sufficiency in food production [9]. The groundwater level in Bangladesh is lowering day by day, as a result of excessive and unsustainable use [6]. These unsustainable practices also pose a serious threat to groundwater contamination [10]. The present pace of extraction, unplanned development, and riverbed silting reduces the lateral influx of surface water to groundwater, causing groundwater availability to worsen [11]. Proper and sustainable management of this natural resource is mandatory, as groundwater sources are limited in nature. Mymensingh is a developing district in Bangladesh. Tremendous pressure on groundwater is experienced in this area, because of the rapid increase in population growth, urbanization, and industrialization [4]. Due to the limitation of surface fresh water sources, people depend on groundwater mainly for their daily water needs and irrigation purposes. The groundwater level has depleted over the past decades in this district, at an average rate of 0.074 m/year [4]. Over-abstraction, poor management, and the effects of climate change are all threatening the long-term viability of groundwater supplies across Bangladesh [12]. In this area, the majority of the tube wells were installed without regard to the hydro-geological features of the aquifers underneath them [13]. This ignorance is currently hampering the performance of tube wells, and the aquifer's potential, because the level of groundwater has dropped below the suction limit. With these tremendous issues, this study aimed to delineate the groundwater potential zones of the Mymensingh district. The study also looked at how advanced technologies, such as remote sensing and geographic information systems (GIS), could be used to assess groundwater potential in a cost-effective and timely manner.

Nowadays, groundwater modelling is considered a very useful tool in groundwater resource management. Researchers from all over the world use a variety of techniques to assess groundwater potential zones, including logistic regression [14], multi-criteria decision analysis [15], frequency ratio [16], weights of evidence [17], decision trees [18], certainty factor [19], Shannon's entropy [20], artificial neural network model [21], and machine learning techniques [22] (i.e., random forest, maximum entropy, and so on), using geological, geophysical, and hydrogeological tools that are typically costly and time-consuming. Remote sensing and GIS are potent instruments that may be used to quickly estimate groundwater resources at a low cost and can be efficiently employed for groundwater research before resorting to more extensive and costly surveying approaches [23]. Many factors are generally responsible for groundwater potential zone development, such as geomorphology, lineament, slope, elevation, soil type, drainage pattern, land use/land cover, rainfall, and so on [24]. A three-step approach, e.g., creating thematic layers, determining the relative importance for each parameter using AHP, and then overlay analysis using GIS can be used to estimate groundwater potential zones [23–26]. Previous research [27–33] assesses groundwater potential zones using RS and GIS methodologies, some including the AHP method [34–36], for sufficiency in decision making. The present study employed RS and GIS methodologies, together with the AHP approach, to map the groundwater potential zones of Bangladesh's north-central area. The findings of the study can be used as a working document to address groundwater concerns in the study area. This document is useful for the industrial and agricultural sectors in selecting work sites and suitable sites for tube well installation. The study's findings will also aid in the implementation of efficient strategies to ensure the sustainable use and extraction of groundwater in this region.

## 2. Materials and Methods

### 2.1. Description of the Study Area

The study area of Mymensingh is in the north-central zone of Bangladesh. Mymensingh district is located at latitudes of 24°15' to 25°12' N and longitudes of 90°04' to 90°49' E. The district has an area of approximately 4396.53 km<sup>2</sup>, with several small valleys between high forests, and accounts for approximately 2.96% of Bangladesh's total area [37], as shown in Figure 1. The city of Mymensingh is located on the bank of the Old Brahmaputra River. In its north-western corner, near Karaibari, the Brahmaputra River enters Mymensingh, then flows towards the south-east and south to the Meghna, near Bhairab Bazar [38]. At a width of 94 m, the Jamuna forms the western edge of Mymensingh, and during the rainy season, this river widens to 5 to 6 m in many areas, while the Meghna flows just over the south-eastern part of the district for a limited distance [39]. Mymensingh has a moderate climate with a humid, oppressive, and mostly cloudy wet season, and a warm, mostly clear dry season [40]. It has a subtropical monsoon climate, with rainfall from May to August and the average annual rainfall is 2541 mm [41]. The region is dominated by recent alluvial flood plain deposits, with underlying Pleistocene Madhupur clay deposits [39]. Mymensingh has a total of 635 perennial bodies of water, covering an area of 49.43 km<sup>2</sup> [42]. Here, the shallow aquifers are characterized by a near-neutral pH, moderate COD, and high arsenic (As) and iron (Fe) levels [4]. The district of Mymensingh is heavily reliant on groundwater. Agricultural irrigation, and other domestic and industrial activities, in this area meet their water needs using groundwater harvesting. Therefore, the decline in the groundwater level has become a vital problem in this area [43].

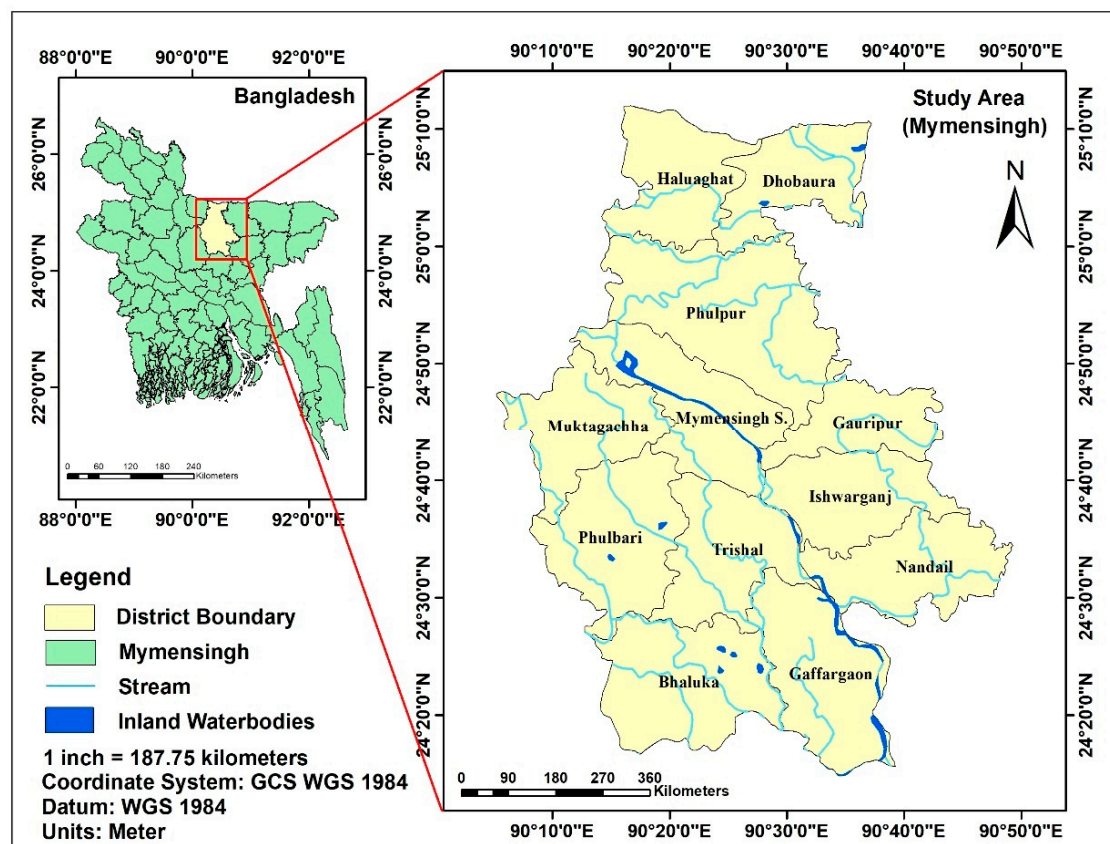


Figure 1. Map of the study area.

### 2.2. Description of Data Processing

Various analogue maps were obtained from various organizations during the early stages of GIS spatial database development (Table 1). Rainfall data was collected from ten

(10) Bangladesh Water Development Board (BWDB) sampling stations for the year of 2020, and interpolated into the GIS system. The soil map was prepared from the “digital soil map of the world” published by the Food and Agriculture Organization (FAO).

**Table 1.** Types of data, data sources, and output layers.

Data Type	Source	Output Layer
DEM (13 June 2019)	ASTER Global Digital Elevation Model V3, NASA	Drainage density, slope, elevation map
Landsat 8 (27 December 2020)	USGS	Land use/land cover, lineament density map
Daily Rainfall Data (Year 2020)	Bangladesh Water Development Board (BWDB)	Annual rainfall map
Geomorphology (2001)	Geological Survey of Bangladesh (GSB)	Geomorphological map
Well Yield & Depth Data (year 2019–2020)	Bangladesh Water Development Board (BWDB) & Water Resources Planning Organization (WARPO)	Used to validate the groundwater potential zones map

Land use, land cover and lineament density data were generated from downloaded Landsat-8 imagery from the USGS Earth Resource Observation System Data Center [<https://earthexplorer.usgs.gov> (accessed on 7 February 2021)]. The map of land use and land cover was generated using supervised classification based on non-parametric rules, and then a theoretical confusion matrix (error matrix) analysis [44] was performed to confirm accuracy using Google Earth and Google Maps, as shown in Table 2.

**Table 2.** Theoretical error matrix of LULC classification.

Parameters	(1)	(2)	(3)	(4)	(5)	Total	Correct Sampled
(1) Agricultural Land	14	0	0	0	0	14	14
(2) Fallow Land	0	11	0	0	0	11	11
(3) Settlement	0	0	10	0	0	10	10
(4) Vegetation	0	0	1	17	0	18	17
(5) Waterbodies	0	0	0	13	1	14	1
Total	14	11	11	30	1	67	53

Final accuracy of LULC classification was evaluated by the following Equation [44]: Accuracy (%) = number of correct sampled/total number of samples =  $(53/67) \times 100 = 79.10\%$

Multi-software processing of Landsat-8 data was used to create a lineament density map. The lineament of the research area was initially derived from Landsat-8 data (Band-04) in PCI Geomatics (demo version). Then, using ArcGIS’ spatial analysis tool, a map of lineament density ( $\text{km}/\text{km}^2$ ) was created. All images were downloaded at level 1 geotiff format, and have a  $30 \times 30$  m spatial resolution, without the presence of cloud cover (4.17%). A geomorphological map of the study area was prepared from the “Quadrangle Map” published by the Geological Survey of Bangladesh (GSB), by digitizing and geo-referencing.

The drainage density map, elevation map, and slope map were prepared from the ASTER Global Digital Elevation Model V3 (DEM), with  $30 \times 30$  m spatial resolution, available on the Earth data site of NASA. The model was validated using well yield data from the Bangladesh Water Development Board’s (BWDB) eight (08) sampling stations. Various analyses and interpretations (digitization, conversion, interpolation, classification, reclassification, enhancement, filtering, and other GIS processing) of satellite data were performed to produce thematic maps in a GIS environment. Lineament density, drainage density, slope, soil, rainfall, elevation, geomorphology, and land use/land cover were all the layers derived from this 3-stage method of groundwater potential zone mapping.

For groundwater potential zone mapping, at first, all data layers were transformed to raster data, with the same  $30 \times 30$  m spatial resolution. A pair-wise comparison was

carried out among all the parameters, to determine the relative importance for groundwater potentiality of each parameter [45]. Each map was reclassified based upon those weights generated. Finally, a groundwater potential map was created by combining all the thematic layers using Arc GIS 10.8's weightage overlay module. A detailed examination of procedures used in this study is illustrated in Figure 2.

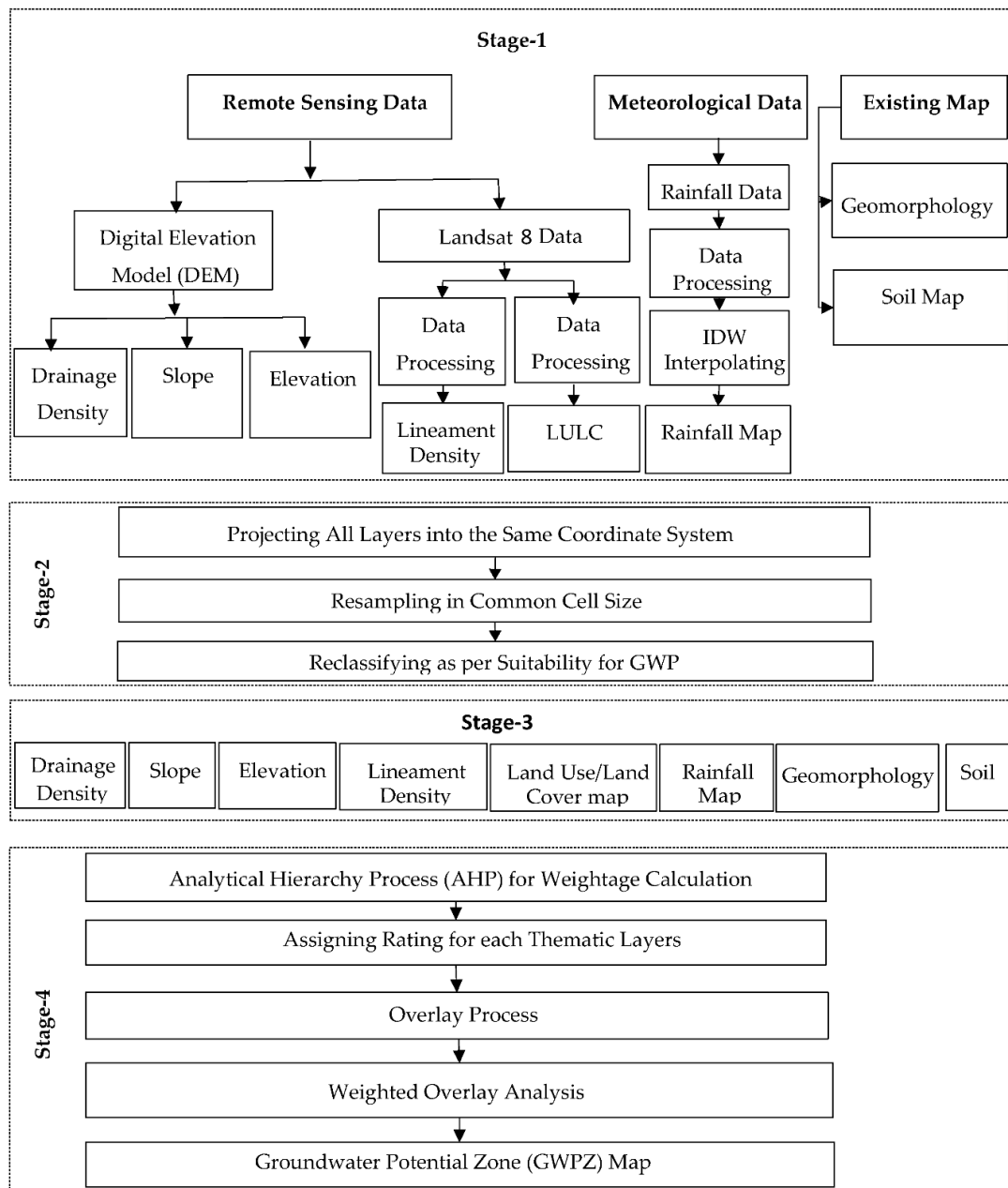


**Figure 2.** Flowchart demonstrating the approaches for mapping groundwater potential zones.

### 2.3. Assigning Weight Using Multi-Criteria Decision Making Approach

Using AHP, a multi-criteria decision-making approach, it is possible to establish the relative importance of various thematic layers and their associated attributes [35,46]. This AHP approach employs the hierarchy to look at many attributes individually, in order to identify possible groundwater flow and storage regulators from competing parameters [36]. The importance of each parameter was graded on a scale of 1 to 9, using a pairwise comparison matrix.

### 2.3.1. Weight Assessment

The weighting of all the influencing parameters was based on their reaction to the occurrence of groundwater and expert opinion [28]. A parameter with a high weight indicates a large influence on groundwater potential, whereas a parameter with a low weight represents a minor impact [47]. Each parameter's weightage was allocated using Saaty's scale of relative importance, with values of 1 to 9 [48–51]. Then, the weights were allocated based on previous studies, together with field experience. According to Saaty's relative importance scale, a value of 1 means equal importance, 2 weak, 3 moderate, 4 moderate plus, 5 strong, 6 strong plus, 7 very strong, 8 very strong plus, and 9 indicates extreme importance [50,51]. Relative weights are ascribed to each thematic layer, based on their categorization, as shown in Table 3.

**Table 3.** Relative weight for selected thematic layers.

Factors	(1)	(2)	(3)	(4)	(5)	(6)	(7)	(8)
(1) Lineament Density	1	2	4	5	6	7	8	9
(2) Slope	0.50	1	2	4	5	6	7	8
(3) Rainfall	0.25	0.50	1	2	4	5	6	7
(4) Drainage Density	0.20	0.25	0.50	1	2	4	5	6
(5) LULC	0.17	0.2	0.25	0.50	1	2	4	5
(6) Geomorphology	0.14	0.17	0.20	0.25	0.50	1	2	4
(7) Soil	0.13	0.14	0.17	0.20	0.25	0.50	1	2
(8) Elevation	0.11	0.13	0.14	0.17	0.20	0.25	0.50	1
Total	2.5	4.39	8.26	13.12	18.95	25.75	33.5	42

### 2.3.2. Weight Normalization

Each row's weights were averaged to find the appropriate ranking, resulting in the normalized weight of each parameter, as shown in Table 4. Based on the study's findings, observed lineament density has a higher value than any other metric. Substantial lineament density indicates the prospect for high groundwater recharge, while low lineament density implies low groundwater recharge, and a low groundwater potential zone. There are more elements that affect GWPZ, listed in increasing order: lineament density > slope > rainfall > drainage density > land use/land cover > geomorphology > soil > elevation.

**Table 4.** Pairwise Comparison Matrix and Normalized Weight.

Factors	(1)	(2)	(3)	(4)	(5)	(6)	(7)	(8)	Weightage	Weightage (%)
(1) Lineament Density	0.4	0.456	0.484	0.381	0.317	0.272	0.239	0.214	0.345	34.53
(2) Slope	0.2	0.228	0.242	0.305	0.264	0.233	0.209	0.19	0.234	23.39
(3) Rainfall	0.1	0.114	0.121	0.152	0.211	0.194	0.179	0.167	0.155	15.48
(4) Drainage Density	0.08	0.057	0.061	0.076	0.106	0.155	0.149	0.143	0.103	10.33
(5) LULC	0.068	0.046	0.03	0.038	0.053	0.078	0.119	0.119	0.069	6.89
(6) Geomorphology	0.056	0.039	0.024	0.019	0.026	0.039	0.06	0.095	0.045	4.48
(7) Soil	0.052	0.032	0.021	0.015	0.013	0.019	0.03	0.048	0.029	2.87
(8) Elevation	0.044	0.03	0.017	0.013	0.011	0.01	0.015	0.024	0.02	2.03
Total	1	1	1	1	1	1	1	1	1	100

### 2.3.3. Principal Eigen Vector

Using the algorithm for the consistency index, the maximum normalized main Eigen vector values (max) were calculated for each parameter, given in Table 5. As examples, lineament density = 34.53 was multiplied by the total value determined within a pairwise comparison matrix (e.g., lineament density = 2.50), shown in Table 4, to obtain the weight of the first criteria. The remaining eight parameters were treated in the same way. Table 5 shows the major eigen vector values (max = 8.527) for determining the consistency index (CI), by adding these values together.

**Table 5.** Normalized Principal Eigen Vectors.

Parameters	Normalized Principal Eigen Vectors
Lineament density	8.948
Slope	9.021
Rainfall	8.915
Drainage density	8.622
LULC	8.293
Geomorphology	8.086
Soil	8.112
Elevation	8.221
$\lambda_{max}$	8.527

### 2.3.4. Consistency Index (CI) and Consistency Ratio (CR) Calculation

The consistency ratio was calculated to evaluate the appropriateness of the weights applied to each parameter. For the weight to be considered constant, the consistency ratio must be less than 0.10. Consistency ratio (CR) was calculated using the following Equation (1) [50]:

$$CR = \frac{CI}{RI} \quad (1)$$

where CI is the consistency index, and RI is the random index. For the present research, the random index value is 1.41, since eight parameters were employed, as per Table 6 [50]. The consistency index was calculated using the following Equation (2):

$$CI = \frac{\lambda_{max} - n}{n - 1} \quad (2)$$

where  $\lambda_{max}$  is the principal eigenvalue of the comparison matrix, and n is the total parameters used in this study.

**Table 6.** Random Index (RI) values for “n” parameters.

n	1	2	3	4	5	6	7	8	9
RI	0	0	0.58	0.92	1.12	1.24	1.32	1.41	1.45

The consistency ratio was calculated to evaluate the appropriateness of the weights applied to each parameter. For the weight to be considered constant, the consistency ratio must be less than 0.10. From the calculation, the consistency index (CI) value is 0.07532. The consistency ratio (CR) result is 0.0538, which is less than 0.1, which means that the given weight for each parameter is valid for further analysis.

The final weightages (percentages) for the weighted overlay analysis are 34.53, 23.49, 15.48, 10.33, 6.89, 4.48, 2.87, and 2.03 for lineament density, slope, rainfall, drainage density, land use/land cover, geomorphology, soil, and elevation, respectively, as the output from multicriteria decision making approaches (AHP), shown in Table 4.

### 2.3.5. Assigning Ratings for the Weighted Overlay Analysis

Appropriate ratings for the overlay approach were assigned based on the influence of each thematic layer, and their classes on groundwater potentiality. The ratings were developed using expert opinion, field study, and previous groundwater potential zone mapping studies. Ratings were assigned on a scale of 1 to 5, with 1 indicating very little influence, and 5 indicating very significant influence.

If lineament density is high in a region, groundwater potential is also high. As a result, regions with lineament density of 0.96 to 1.78 km/km<sup>2</sup> are assigned a 5 (very high) rating, as these areas have long, major faults. Another rating, 4 (high), is given to the lineament density showing local faults that are linked together (frequent faults). A

rating of 3, 2, and 1 is given for 0.49–0.96 km/km<sup>2</sup>, 0.28–0.49 km/km<sup>2</sup>, 0 to 0.28 km/km<sup>2</sup> lineament density, respectively. In the research region, slopes are classified as very low (0–10), low (1–20), moderate (2–30), high (3–50), and very high (>50) slopes. Flat slopes receive the highest rating (very low) because they hold water for a long period, allowing groundwater to easily refill through infiltration. The steep (very high) slope is assigned the lowest ranking, because it causes a lot of runoff and minimal groundwater recharge. The availability of water for infiltration is increased when the yearly rainfall is high. So, locations with 2443–2634 mm/year rainfall receive a high grade of 5. As a result, areas with annual rainfall between 2316 and 2442 mm, 2208 to 2315 mm, 2106 to 2207 mm, and 1964 to 2106 mm are assigned a rating of 4, 3, 2, and 1, respectively. As a high drainage density area causes more surface runoff, the region with the highest drainage density (1.98 to 3.18 km/km<sup>2</sup>) receives the lowest rating of 1. As a result, high, moderate, low, and very low drainage density receive ratings of 2, 3, 4, and 5, respectively, as shown in Table 6. The ratings for land use and land cover are based on the quantity of water available for recharging, depending on the landform. Agricultural land and bodies of water are assigned the highest rating of 5, paved settlement areas receive the lowest grade of 1, and vegetation area has a rating of 3. For its low permeability, fallow land receives a rating of 2. There are several geomorphologies in this research area. Madhupur clay residuum is given a rating of 2, as these areas are less suitable for groundwater recharge. Young gravelly sand, lakes, and the Chandina alluvium floodplain all obtain a rating 5, since these formations are well-known for effective groundwater recharging. Alluvial silt, and alluvial silt and clay are rated 4 and 3, respectively. Marsh clay and peat, and the Dihing and Dupi Tila formation undivided are assigned a rating of 1, due to relatively lower permeability. Depending on the characteristics, the soil groups of Dystric Nitosols (Nd) are assigned the maximum rating of 5, while Eutric Gleysols (Ge), with greater silt and clay, receive the lowest rating of 4. The elevation value ranges from 3 to 12 m, receiving the maximum rating of 5, indicating that it is more likely to recharge groundwater. Based on their appropriateness for groundwater potential, elevations ranging from 12 to 15, 15 to 20, 20 to 27, and 27 to 75 m are assigned ratings of 4, 3, 2, and 1, respectively. Table 6 represents the weights and the ratings (rank) of the eight criteria with their area coverage (km<sup>2</sup>). Table 7 depicts the list of parameters, together with their assigned weights, ratings, and area coverage.

**Table 7.** A list of parameters, together with their assigned weights, ratings, and area coverage.

Influence/Weightage (%)	Class	GWSP	Ratings	Area Coverage (km <sup>2</sup> )
Lineament Density (km/km <sup>2</sup> )				
34.53	No lineament (0–0.28)	Very low	1	916.714
	Fractures, short lineament (0.28–0.49)	Low	2	1317.58
	Local faults, frequent fractures (0.49–0.70)	Moderate	3	1113.2
	Interconnected local faults, frequent faults (0.70–0.96)	High	4	741.212
	Major long faults (0.96–1.78)	Very high	5	263.522
Slope (Degree)				
23.39	0–1°	Very high	5	1707.94
	1–2°	High	4	993.931
	2–3°	Moderate	3	651.151
	3–5°	Low	2	688.963
	>5°	Very low	1	295.438
15.48	1964–2106	Very low	1	759.143
	2106–2207	Low	2	1134.4
	2208–2315	Moderate	3	992.733
	2316–2442	High	4	1115.09
	2443–2634	Very high	5	351.268

Table 7. Cont.

Influence/Weightage (%)	Class	GWSP	Ratings Area Coverage (km <sup>2</sup> )	
Rainfall (mm/year)				
Drainage Density (km/km <sup>2</sup> )				
10.33	Very low density (0–0.83)	Very high	5	416.202
	Low density (0.83–1.20)	High	4	1319.48
	Moderate density (1.20–1.48)	Moderate	3	1683.34
	High density (1.48–1.98)	Low	2	823.131
	Very high density (1.98–3.18)	Very low	1	110.13
LULC				
6.89	Waterbodies	Very high	5	582.07
	Vegetation	Moderate	3	1403.19
	Agricultural land	Very high	5	1887.27
	Fallow land	Low	2	146.276
	Settlement	Very low	1	333.469
Geology				
4.49	Young gravelly sand	Very high	5	322.001
	Marsh clay and peat	Very low	1	639.124
	Madhupur clay residuum	Low	2	704.856
	Lakes	Very high	5	17.1666
	Dihing and Dupi Tila formation undivided	Very low	1	40.8996
	Chandina alluvium	Very high	5	1188.56
	Alluvial silt and clay	Moderate	3	559.128
	Alluvial silt	High	4	871.687
	Unmapped area	Very low	1	8.8065
Soil				
2.87	Eutric Gleysols	High	4	3170.69
	Dystric Nitosols	Very high	5	1167.25
Elevation (meters)				
2.03	3–12	Very high	5	2210.89
	12–15	High	4	1313.39
	15–20	Moderate	3	681.433
	20–27	Low	2	132.174
	27–75	Very low	1	14.4003

### 2.3.6. Weighted Overlay Analysis for Groundwater Potential Zone Mapping

Weighted overlay analysis [52] is an approach for generating an extensive analysis, by assigning a common scale of values to input components based on AHP analysis. Each input layer was reclassified to a common ratio scale of five specific classes. Using the weighted overlay tool of ArcGIS 10.8 software, the reclassified layers of lineament density, drainage density, slope, soil, rainfall, elevation, geomorphology, and land use/land cover, and their corresponding percentage influence on recharge, were integrated to produce a map of the spatial distribution of groundwater potentials within the Mymensingh district. By multiplying the cell values of each factor class by the factor weight, and summing the resulting cell values together, the weighted overlay analysis tool reclassified values in the input raster layers into a common evaluation scale of 1, 2, 3, 4, and 5; very low, low, moderate, high, and very high, respectively. The following Equation (1) [28,29,31,47,52] was used to measure ground water potential zones of the study area:

$$\begin{aligned}
 \text{GWPZ} = & (\text{Rfw}) \times (\text{Rfr}) + (\text{Gew}) \times (\text{Ger}) + (\text{Slw}) \times (\text{Slr}) \\
 & + (\text{DDw}) \times (\text{DDr}) + (\text{LDw}) \times (\text{LDr}) + (\text{Sw}) \times (\text{Sr}) \\
 & + (\text{LULCw}) \times (\text{LULCr}) + (\text{Elw}) \times (\text{Elr})
 \end{aligned} \quad (3)$$

where Rf = rainfall; Ge = geomorphology; Sl = slope; DD = drainage density; El = elevation; S = soil; LULC = land use/land cover; and LD = lineament density. The symbol “w” expresses the weightage of a thematic layer, and the symbol “r” expresses the rating of subclasses (the rank) in each layer.

#### 2.4. Validation of Results

One of the most important criteria in scientific study is validation. The defined GWPZs were validated using the well yield of pump test data obtained from the Bangladesh Water Development Board (BWDB). Cross-verification analysis [53] was performed between the groundwater potential zone values and well yield data. A total of 8 well yield data (liter per second) were found and used for the investigation.

Again, we used groundwater depth data acquired from the monitoring wells of the Bangladesh Water Development Board (BWDB), and the Water Resources Planning Organization (WARPO), for the years 2019 and 2020, to validate our findings. A total of 68 monitoring well data points were obtained and interpolated in GIS, using the kriging interpolation method. Then, an accuracy assessment was performed using confusion matrix (error matrix) analysis between the resulting groundwater potential zones map and the observation wells data. The observation wells data were used as a point of reference for determining the accuracy of classification. The total accuracy was calculated using the following equation [54,55]:

$$\text{Accuracy (\%)} = (\text{number of correct sampled} / \text{total number of samples}) \times 100 \quad (4)$$

Then, kappa (K) analysis [56] was used, which is a multivariate way to evaluate accuracy that yields a Khat statistic. It was determined by applying the following equation [56,57]:

$$\text{Kappa Coefficient (T)} = \frac{(\text{TS} \times \text{TCS}) - \sum (\text{Column Total} \times \text{Row Total})}{\text{TS}^2 - \sum (\text{Column Total} \times \text{Row Total})} \times 100 \quad (5)$$

where TS stands for total samples, and TCS stands for total correct sampled.

### 3. Results

#### 3.1. Description of Influential Factors

Thematic maps were prepared at a scale of 1:50,000, with a spatial resolution of 30 × 30 m from satellite imagery, geomorphological mapping, soil mapping, and other hydrogeological field data. Thematic maps for each parameter are prepared as follows:

##### 3.1.1. Lineament Density

Lineament density in the study area ranges from 0 km/km<sup>2</sup> to 1.78 km/km<sup>2</sup>. The region is divided into five classifications to make it easier to provide a rating. Potentiality of groundwater depends largely on lineament density because it helps in groundwater recharge [57]. When the lineament density in an area is high, the potentiality of groundwater is also high. So, the rating of 5 (very high) is given to areas with a lineament density of 0.96 to 1.78 km/km<sup>2</sup>. This is because these areas have long, major faults. A little more than 6.05% of the area is covered by this class. Another rating, 4 (high), is given to the lineament density showing local faults that are linked together. It covers 17.03% of the study area, and has a value of 0.70 to 0.96 km/km<sup>2</sup> (frequent faults). In the middle of the scale, the lineament density ranges from 0.49 km/km<sup>2</sup> to 0.70 km/km<sup>2</sup>. Almost 25.68% of the research region is in this classification, and so this class receives a rating of 3, as it shows local faults with a lot of fractures. A total of 30.27% of the area has lineament density of 0.28–0.49 km/km<sup>2</sup> or less, which is assigned a rating of 2, because it shows fractures with short lines. Lineament density in these areas from 0 to 0.28 km/km<sup>2</sup>, covering about 21% of the total study area, receives a rating of 1. Lineament density is assigned 34.53% of the weight. Figure 3A shows lineament density in the study area.

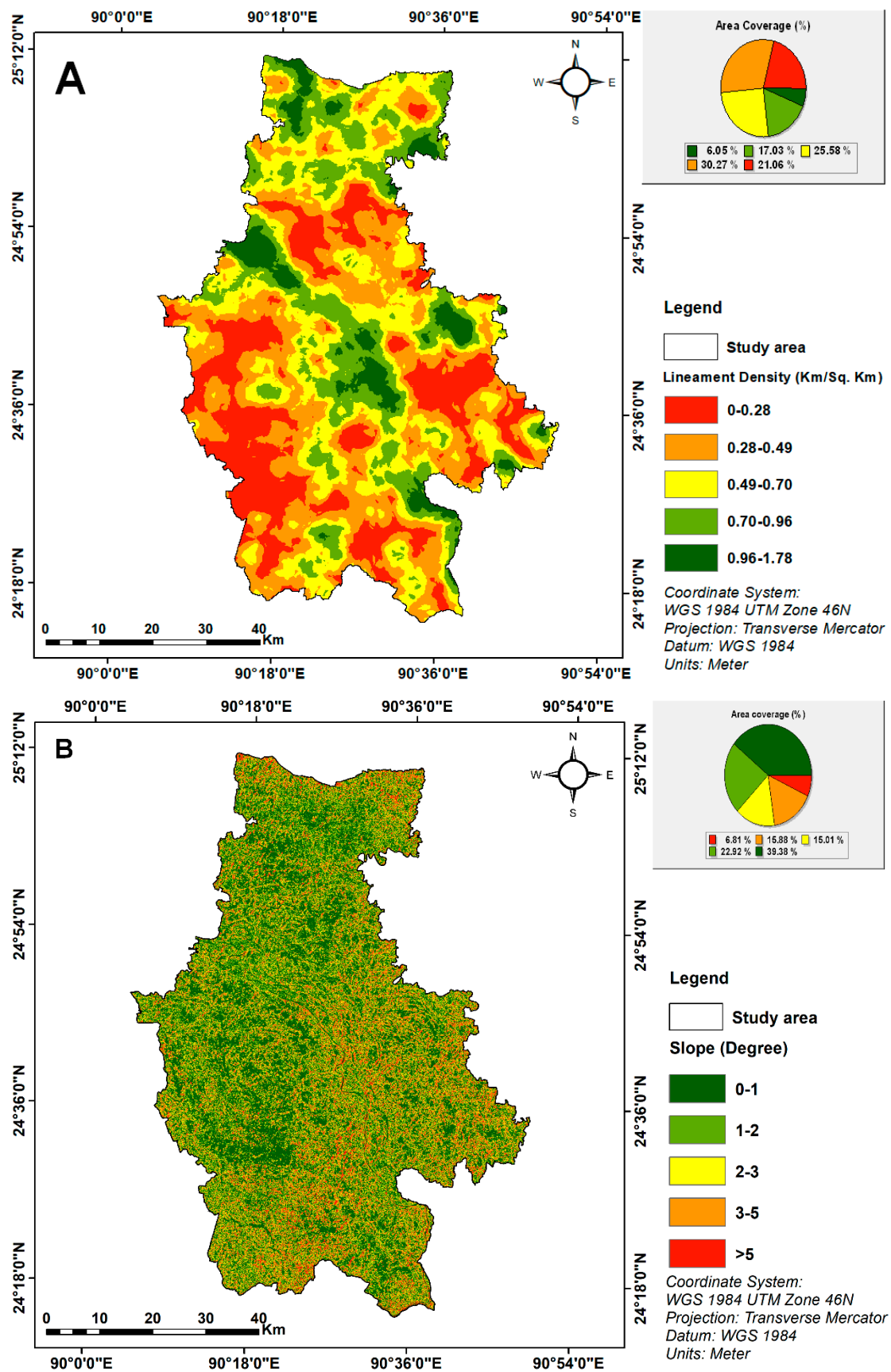


Figure 3. Cont.

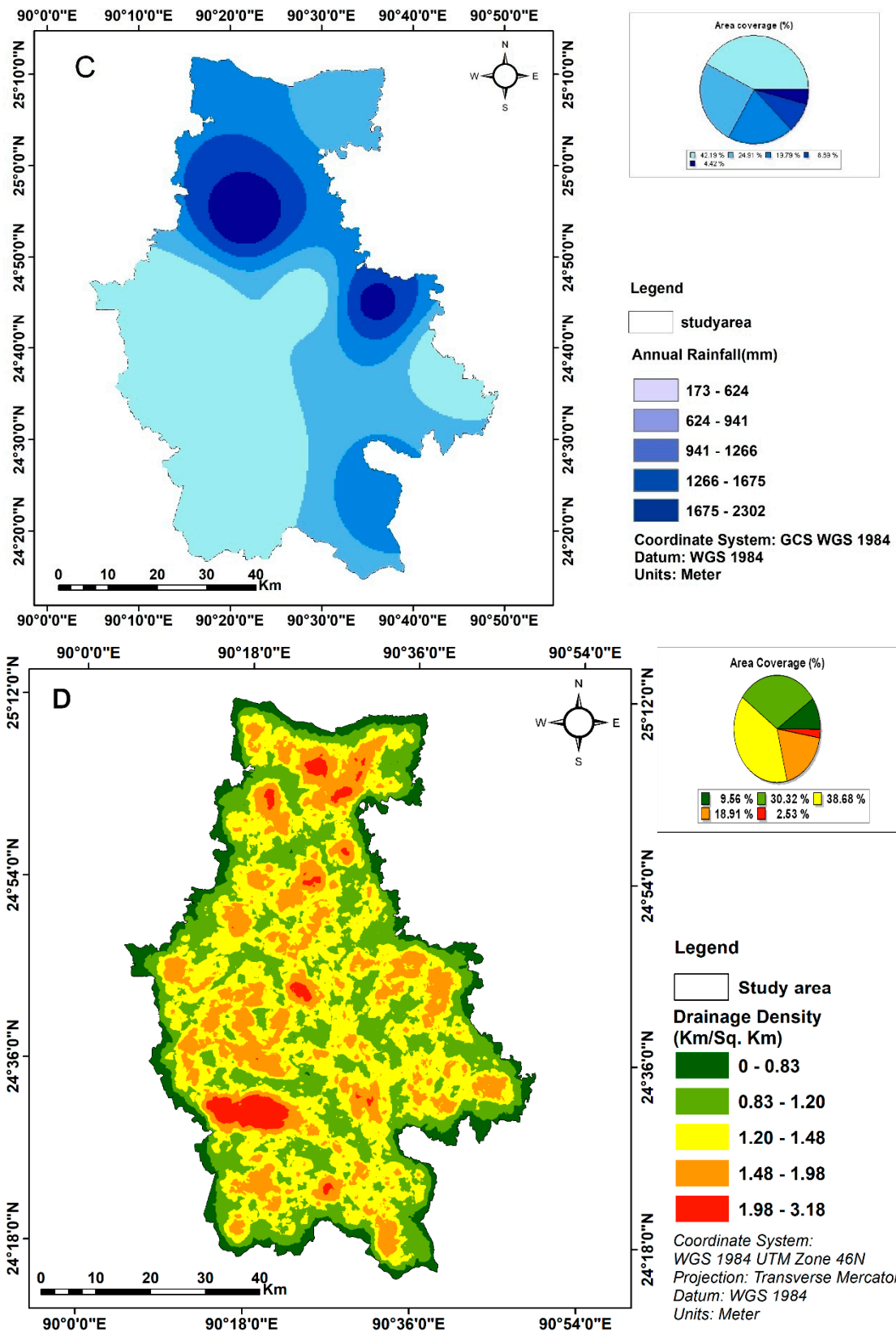


Figure 3. Cont.

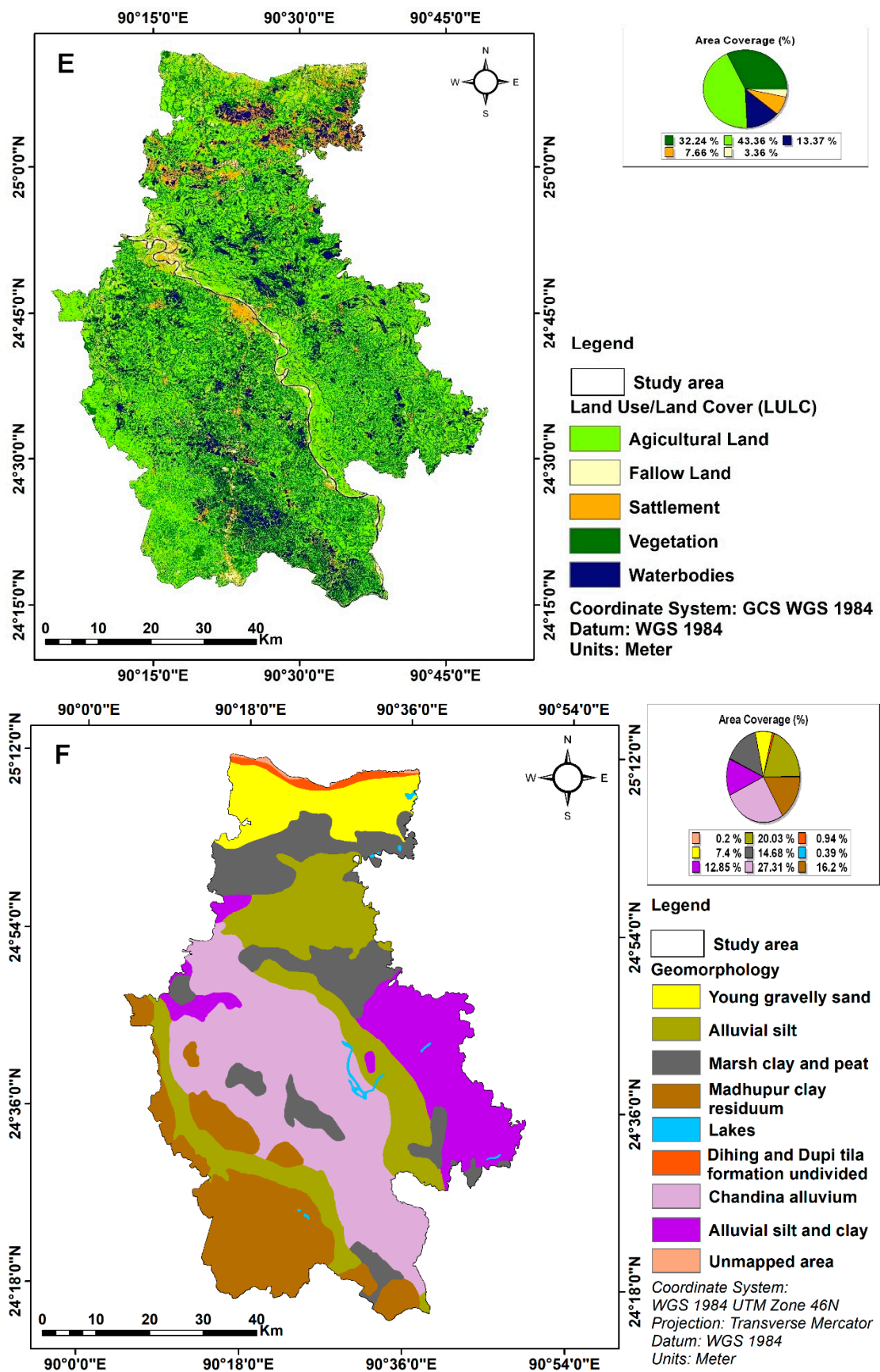
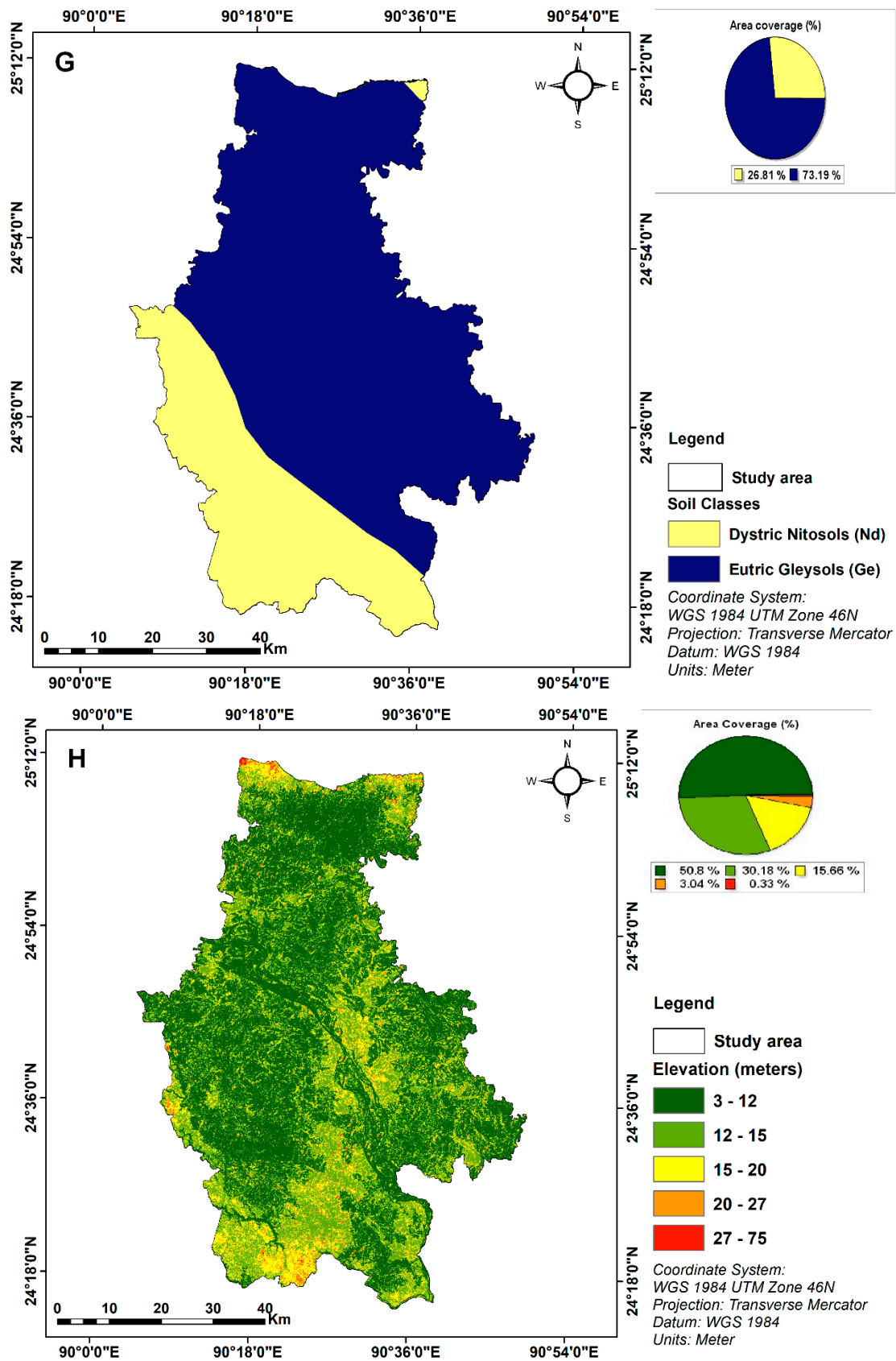


Figure 3. Cont.



**Figure 3.** Lineament density of the study area (A); slope of the study area (B); annual rainfall map of the study area (C); drainage density map of the study area (D); LULC map of the study area (E); geomorphology map of the study area (F); soil texture of the study area (G); elevation map of the study area (H).

### 3.1.2. Slope

Slope categorization in the study area is categorized as very low ( $0-1^\circ$ ), low ( $1-2^\circ$ ), moderate ( $2-3^\circ$ ) slopes, as well as high ( $3-5^\circ$ ) and very high ( $>5^\circ$ ) slopes. Figure 3B shows the reclassified slope map of the study area. The highest rating is assigned to flat slopes (very low), because they hold water for a long time, meaning that groundwater is easily refilled by infiltration [58]. The lowest rank is given to steep (very high) slopes because they cause a lot of runoff and little groundwater recharge. A total of 39.38% of the study area is flat land with very little slope, 15.10% is medium slope, and 6.81% is very steep slope.

### 3.1.3. Rainfall

Rainfall is the most important source of water in the water cycle, as well as one of the most influential factors for groundwater availability. Rainfall intensity and duration have a big impact on how much water is infiltrated, and how much water runs off [59]. The hydrology of the study area mainly depends on monsoon rainfall [12]. Table 8 depicts the study area's yearly rainfall for the year 2020. The amount of rain that falls inside the north and north-east highland parts of the study area directly affect the rate at which groundwater is infiltrated in the central downstream area. The rainfall map of the study area is shown in Figure 3C.

**Table 8.** Annual rainfall data of the study area.

Area	Annual Rainfall (mm/year)	Area Coverage (%)
Western and south-western part	1964–2106	17.44
Central part	2106–2207	26.06
Northwestern and south-eastern part	2208–2315	22.81
Southeastern and north-western part	2316–2442	25.62
Northern and north-eastern part	2443–2634	8.07

### 3.1.4. Drainage Density

Drainage density is connected to permeability, which affects how much water runs off, and how much water soaks into the ground [60]. The drainage density is classified into five categories: very high, high, moderate, low, and very low drainage density zone, as illustrated in Figure 3D. The drainage density in the study area ranges from 0 to 3.18 km/km<sup>2</sup>. Approximately 9.56% of the overall land has a relatively low drainage density. Only 2.53% of the study area has a very high drainage density, ranging from 1.98 to 3.18 km/km<sup>2</sup>. Compared to a low drainage density region, a high drainage density area increases surface runoff. The maximum drainage density number reflects the greatest possibility of runoff, which eventually leads to less percolation. As a result, the lowest rating of 1 is given to the region with the highest drainage density, and a rating of 5 is given to the region with the lowest drainage density, 0 to 0.83 km/km<sup>2</sup>.

### 3.1.5. Land Use/Land Cover

The land use type of the study region determines information on soil moisture, permeability, amount of runoff, and percolation [61]. Mymensingh is a semi-urban region comprised of 43.38% of agricultural land, 3.36% of fallow land, 13.37% of water body mask, 7.64% of settlements, and 32.24% of vegetation, according to the LULC map, shown in Figure 3E. According to the results of the theoretical confusion matrix (error matrix) analysis, the LULC map has an accuracy of 79.10%, suggesting that the classified image is appropriate for further investigation. The ratings are assigned based on the amount of water available for recharging, depending on the landform. Agricultural land and waterbodies receive the maximum rating of 5, while paved settlement areas receive the lowest rating of 1, and vegetation area has a rating of 3. Fallow land receives a rating 2 due to its limited permeability. This layer is assigned a weight of 6.89%.

### 3.1.6. Geomorphology

The features of various water-bearing geomorphological formations influence the occurrence and flow of groundwater [62]. In this area, there are nine major geomorphologies: young gravelly sand, marsh clay and peat, Madhupur clay residue, lakes, Dihing and Dupi Tila formation undivided, Chandina alluvium, alluvial silt, alluvial silt and clay. Here, Madhupur clay residuum underlays 16.02% of the entire area, which is assigned a rating of 2, since these locations do not favor groundwater recharging. Young gravelly sand (7.4%), lakes (0.39%), and the Chandina alluvium floodplain (27.31%) each receive a rating of 5, as these formations are well-recognized for efficient groundwater recharge, and the Chandina alluvium floodplain occupies the majority of the research region. Alluvial silt (20.03%) and alluvial silt and clay (12.85%) have ratings of 4 and 3, respectively. Marsh clay and peat (14.68%) and Dihing and Dupi Tila formation undivided (0.94%) receive a rating of 1, due to extremely low permeability. This thematic layer is assigned a weight of 4.49%. Figure 3F shows the geomorphology map of the study area.

### 3.1.7. Soil Texture

The rate of infiltration is determined by the uppermost soil's permeability and water holding capacity [63]. Figure 3G shows the different types of hydrogeological soils classes in the study area. The largest part (73.19%) of the study area, is made up of Eutric Gleysols (Ge), with silty characteristics (containing mainly silt and clay). Another 26.81% of the region consists of Dystric Nitosols (Nd), with sandy characteristics. Depending on the characteristics, the highest rating of 5 is assigned to the soil groups of Dystric Nitosols (Nd), while the lower rating of 4 is assigned to Eutric Gleysols (Ge) with higher silt and clay. The overall weight for this layer is 2.87%.

### 3.1.8. Elevation

The elevation of the land is an essential aspect of groundwater recharge. Plains with lower altitudes tend to retain water longer, resulting in higher groundwater recharge [64]. Inside the northern and southern parts of the area, there are many big hills. Figure 3H shows that the elevation inside the study ranges from 3 to 75 m. The elevation is higher in the northern and southern parts of the study area. A total of 50.80% of the study area has elevation values of 3 to 12 m, and receives the highest rating, 5, as it is more likely to allow groundwater recharge. As follows, 12 to 15, 15 to 20, 20 to 27, and 27 to 75 m elevation, covering 30.18%, 15.66%, 3.04%, and 0.33% of the study area, respectively, are assigned the ratings of 4, 3, 2, and 1, based on their suitability for groundwater potential. The overall weight for this layer is 2.03%.

## 3.2. Groundwater Potential Zone

The eight thematic layers were generated in a GIS context, and the applicable rankings and weights, decided by the AHP technique, were allocated to them for the overlay analysis by combining all thematic maps. The findings are classified into five groups, based on the total values generated from Equation (3), ranging from very low potential zones to very high potential zones (Figure 4). The values of groundwater potential zones range from 4.49 to 338.50. Natural breaks classification is used to classify this groundwater potential zones (Table 9).

**Table 9.** Groundwater potential zonation with area coverage.

GW Potentiality	Area Coverage (km <sup>2</sup> )	Area Coverage (%)
Very low	235.17	5.37
Low	1176.84	26.88
Moderate	1466.46	33.50
High	995.58	22.74
Very high	504.09	11.51

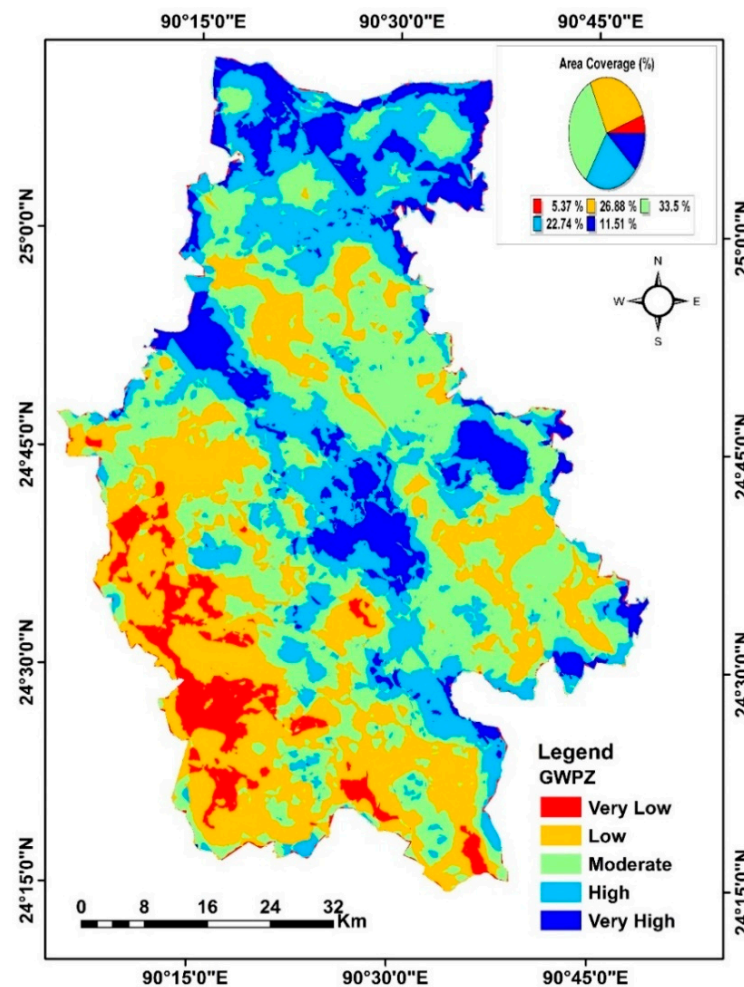


Figure 4. Groundwater potential zone of the study area.

Due to the flat surface of the research area, there is a higher likelihood of groundwater recharge. The northern, north-eastern, and central parts of the research area, all of which are inundated by water, have a greater possibility of having a zone of very high to high potential, covering 11.51% (504.09 km<sup>2</sup>) and 22.74% of the study area, respectively (995.58 km<sup>2</sup>). Areas where lineament density is higher, but the drainage density is lower, result in increased groundwater potentiality. Furthermore, in areas with low rainfall intensity and high drainage density, all of the water flows away, with little time to recharge the groundwater. In these locations, 5.375% (235.17 km<sup>2</sup>) and 26.88% (1176.84 km<sup>2</sup>) are classified as having very low to somewhat low potential zones. The eastern half of the research area has a low to moderate potential zone, with moderate rainfall, lineament, slope, and drainage density. A moderate potential zone, with an extent of up to 33.50%, covers the majority of the research area (1466.46 km<sup>2</sup>).

### 3.3. Validation of Groundwater Potential Zone

Cross-verification [53,64] was performed between the groundwater potential zone map and well yield data from the BWDB. A total of eight well yield data were found and used for the investigation, and their water production (liter per second) was extrapolated from the measured data. Well yield production (liter per second) varies from 25.21 to 37.56. This groundwater potential zone is in close (87.5%) accord with the results of the point source data provided in Table 10. High-yielding groundwater is found in several locations of the country. Rift faults in the region are likely responsible for this, since they may have created a range of degrees of displacement within rock formations that are now in touch with high-permeability rock types [62]. It is clear from the table that the findings achieved

using this technique are in excellent agreement with real-time data. Therefore, the findings produced are more in line with the real field data.

**Table 10.** Validation of groundwater potential zone map using well yield data.

Well Id	Latitude (DD)	Longitude (DD)	Yield (LPS)	Expected Yield Description	Actual Yield Description	Agreement between Expected and Actual Yield Description
GA6113004	24.450001	90.370003	28.39	Very low to low	Low	Agree
GA6120008	24.610001	90.339996	28.39	Very low to low	Low	Agree
GA6120018	24.584000	90.256000	28.39	Very low to low	Low	Agree
GA6124003	25.044000	90.382000	25.21	Low to moderate	Very low	Disagree
GA6152017	24.685000	90.378000	28.39	Low to moderate	Low	Agree
GA6165005	24.853000	90.255000	37.86	High to very high	High	Agree
GA6181006	24.977000	90.400000	37.86	High to very high	High	Agree
GA6194016	24.555000	90.437000	28.39	Low to moderate	Low	Agree

Again, we used groundwater depth data acquired from the Bangladesh Water Development Board (BWDB), and the Water Resources Planning Organization (WARPO), for the years 2019 and 2020, to validate study’s findings, as shown in Figure 5. A total of 68 monitoring well data were obtained and interpolated in GIS, using the kriging interpolation method. The average depth of the monitoring well ranges from 3.95 m to 10.37 m.

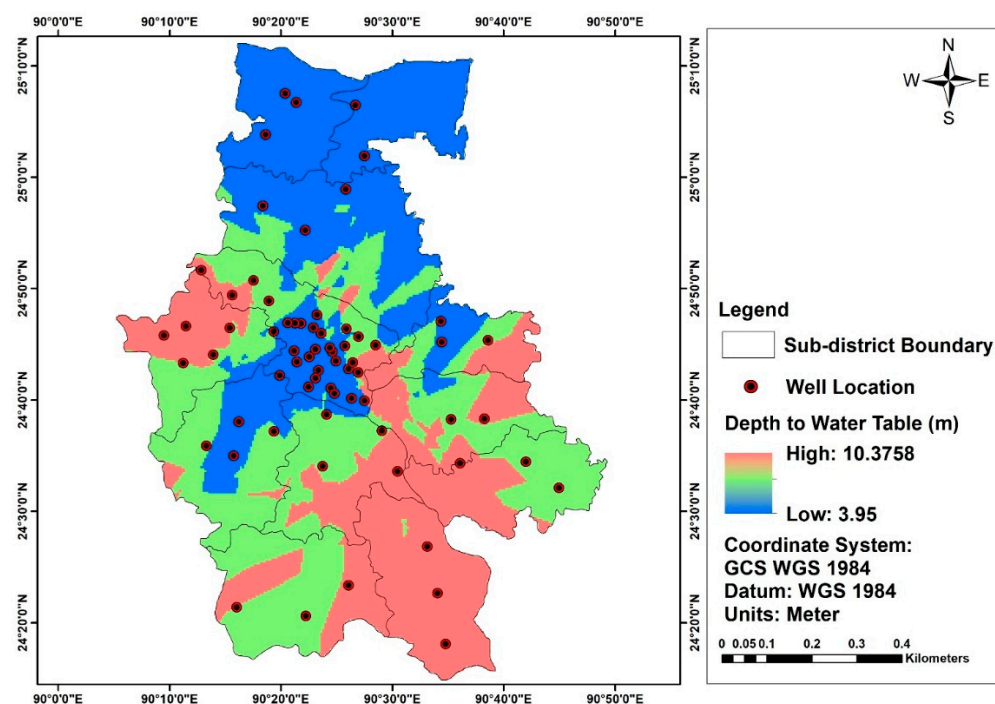


**Figure 5.** Monitoring well locations with the depth to water table in the study area.

An accuracy assessment was performed between the resulting groundwater potential zones map and the observed well data. The observation well data were used as a point of reference for determining accuracy of classification.

A confusion matrix (error matrix) analysis was used to measure accuracy, as shown in Table 11. The total accuracy was calculated using the Equation (4):

$$\text{Accuracy (\%)} = ((59/68) \times 100 = 86.76\%$$

**Table 11.** Theoretical confusion matrix for total accuracy and Kappa coefficient analysis.

GWPZs	(1)	(2)	(3)	(4)	(5)	Total	Correct Sampled
(1) Very low	10	2	1	0	0	13	10
(2) Low	0	11	1	0	0	12	11
(3) Moderate	1	1	8	0	0	10	8
(4) High	0	0	0	13	2	15	13
(5) Very high	0	0	0	1	17	18	17
Total	11	14	10	14	19	68	59

After that, kappa coefficient (T) analysis was used, which is a multivariate way to evaluate accuracy that yields a Khat statistic. It was determined by applying Equation (5):

$$\begin{aligned}
 T &= \frac{(68 \times 59) - \{(13 \times 11) + (12 \times 14) + (10 \times 10) + (15 \times 14) + (18 \times 19)\}}{68^2 - \{(13 \times 11) + (12 \times 14) + (10 \times 10) + (15 \times 14) + (18 \times 19)\}} \times 100 \\
 &= \frac{4012 - 963}{4624 - 963} \times 100 \\
 &= \frac{3049}{3661} \times 100 \\
 &= 83.28\%
 \end{aligned}$$

The total accuracy and kappa coefficients are 86.76% and 83.28%, respectively, with a considerable level of agreement [65], indicating a good connection between groundwater potential zones and actual monitoring well information.

#### 4. Discussion

Groundwater is the most abundant source of potable freshwater, as surface water sources are contaminated, or being contaminated, with anthropogenic contaminants [66–69]. Groundwater depletion is one of the world’s most pressing worries, with the effects felt most acutely in underdeveloped countries [70]. Water consumption has risen dramatically in recent years, as a result of population increase and socioeconomic development [61]. Groundwater modeling is now regarded as a very efficient technique for managing groundwater resources. Groundwater recharge has considerably diminished, almost everywhere in the world, as a result of numerous anthropogenic activities and imbalanced development [71–73]. Knowing where groundwater potential zones are can aid in the more precise study of groundwater resources for sustainable use, as well as in the establishment of artificial groundwater recharge systems [29,74,75]. Groundwater is the principal source of fresh water in Bangladesh, and its agricultural sector is largely dependent on groundwater [76]. Within study region, a divisional city of Bangladesh, great strain on groundwater is experienced, due to the fast population growth, urbanization, and industrialization [77]. In the north-central region of Bangladesh, the majority of the tube wells were installed without regard to the hydrogeological features of the aquifers underneath them. This ignorance is currently hampering the performance of tube wells, because the level of groundwater has dropped below the suction limit [43]. This study analyzed hydrologic and geographic attributes of the north-central region of Bangladesh, covering eight major factors influencing groundwater potential: geomorphology, land use/land cover, drainage density, lineament density, soil type, slope, elevation, and annual rainfall. The hydrogeological information of the study area will help future researchers and policymakers in groundwater resource management. Similar studies for assessing groundwater potential zones were conducted worldwide [23,24,26,28–34,74,78–80], as it is a quick, cost-effective, and reliable way of predicting groundwater potentiality. In Bangladesh, similar studies covering the Atrai-Sib River basin [81], Dhaka city [82], agricultural area in Dinajpur district [83], the hilly terrain of Bangladesh [84], and drought-prone areas of Bangladesh [85] were performed, and no study was conducted in the Mymensingh district for groundwater potentiality. During the last few years, this district experienced intensive industrial activities. Many industries were built in this district, which created excessive pressure on ground water consumption. This study is useful in groundwater management, decision making, and

as a guide for future detailed investigations in the study area. Based on the influence of groundwater potentiality, all the thematic layers were quantitatively placed together using GIS and multicriteria decision making approaches (AHP), and categorized the study area into very high, high, moderate, low, and very low groundwater potential zones. The modeled map was validated by groundwater depth data using a confusion matrix, and kappa coefficient analysis. This study has certain limitations, such as model validation using cross-verification relying on groundwater yield data from BWDB's eight monitoring stations, as there were only eight monitoring stations found from a reliable data source (BWDB) in the study region. To meet this gap, we also employed groundwater depth data from 68 monitoring wells in the study area for validation, using a confusion matrix and kappa coefficient. The total accuracy and kappa coefficients are 86.76% and 83.28%, respectively, with a considerable level of agreement [68,69], indicating a good connection between groundwater potential zones and actual monitoring well information. As per the study's findings, areas with flat surface, higher lineament density, lower drainage density, and higher annual rainfall show higher groundwater potentiality. The findings of the study can be used as a working document to address groundwater concerns in the study area. This document is useful for the industrial and agricultural sectors in selecting work sites and suitable sites for tube well installation. Based on the findings of this study, and earlier research, it is possible to conclude that integrated GIS and remote sensing techniques are immensely helpful, time-efficient, and cost-effective tools for modeling groundwater potential zones. Integrated remote sensing and GIS approaches are highly recommended for rapid, cost-effective, and reliable assessment in groundwater potential zone research.

## 5. Conclusions

At present, groundwater is an essential and valuable resource. The geographic information system (GIS) and remote sensing are remarkable and practical tools, as they are less time consuming and more cost-effective ways to discover groundwater potential zones in any region. In the present study, the analytical hierarchy process (AHP), along with GIS and remote sensing, was used to delineate the groundwater potential zones of the Mymensingh district (the north-central region of Bangladesh), based on the influential factors for groundwater potential zones. This simple and systematic method successfully provides a satisfactory result concerning the delineation of groundwater potential areas. The study results in a groundwater potential zone map for Mymensingh district that identifies that there is a higher potential for about 11.51% of the study area to be a high groundwater potential zone, which is an area of about 504.09 km<sup>2</sup>. The AHP analysis reveals that physiographical parameters, such as lineament density, slope, drainage density, geomorphology, and meteorological factors such as annual rainfall, have greater influence over groundwater potentiality. The groundwater level is depleting alarmingly in the study area, and making a lot of deep and shallow tube wells useless. To manage these valuable resources, we need to reduce our dependency on groundwater, by searching for alternatives. Proper management of groundwater recharge zones is also a very reliable way to enhance these resources. Agricultural activities in the study area directly depend on groundwater. Searching for alternative water resources is keenly needed for sustainable management of groundwater. Dredging the Old Brahmaputra River, and its adjacent canals, could be an important alternative in this regard. This study will help decision making for the sustainable management of groundwater resources, site determination for groundwater investigation, and exploitation. This study will also help develop natural or artificial recharge structures, for the prospect of groundwater use in the Mymensingh district to fulfil their water crisis during the dry season.

**Author Contributions:** Conceptualization, M.A.S. and M.A.I.; methodology, M.A.S., M.A.I., U.P. and M.N.-E.-A.; software, M.A.I., M.N.-E.-A., S.K.S. and U.P.; validation, M.A.S., A.R.M.T.I. and M.F.U.; formal analysis, M.A.I., M.N.-E.-A., S.K.S. and U.P.; investigation, M.A.I. and U.P.; resources, S.I.I., A.R.M.T.I. and M.F.U.; data curation, M.A.S., M.A.I., A.R.M.T.I. and S.K.S.; writing—original draft preparation, U.P., M.A.I., M.N.-E.-A. and M.A.S.; writing—review and editing, A.R.M.T.I., M.F.U., A.E.R. and S.K.S.; visualization, M.A.S., A.R.M.T.I., A.E.R. and S.K.S.; supervision, M.A.S.; project administration, M.A.S.; funding acquisition, M.A.S., A.E.R., M.A.I., M.N.-E.-A., U.P. and S.I.I. All authors have read and agreed to the published version of the manuscript.

**Funding:** The work was supported by grants from the Research Cell, Noakhali Science and Technology University (No: NSTU/RC-ESDM/T-21/56).

**Institutional Review Board Statement:** Not applicable.

**Informed Consent Statement:** Not applicable.

**Data Availability Statement:** Not applicable.

**Acknowledgments:** The authors would like to show gratitude to the GIS Lab of the Department of Environmental Science and Disaster Management, Noakhali Science and Technology University. Thanks are given to the Bangladesh Water Development Board (BWDB) for providing the valuable data for this research. Special thanks to Universiti Malaysia Kelantan (UMK) for providing partial financial support of article processing charge.

**Conflicts of Interest:** The authors declare no conflict of interest.

## References

1. Yamazaki, D.; Trigg, M. The dynamics of Earth's surface water. *Nature* **2016**, *540*, 348–349. [[CrossRef](#)]
2. Al-Manmi, D.A.M.; Rauf, L.F. Groundwater potential mapping using remote sensing and GIS-based, in Halabja City, Kurdi-stan, Iraq. *Arab. J. Geosci.* **2016**, *9*, 357. [[CrossRef](#)]
3. Manap, M.A.; Nampak, H.; Pradhan, B.; Lee, S.; Sulaiman, W.N.A.; Ramli, M.F. Application of probabilistic-based frequency ratio model in groundwater potential mapping using remote sensing data and GIS. *Arab. J. Geosci.* **2012**, *7*, 711–724. [[CrossRef](#)]
4. Basunia, Z.A.; Hossain, M.A.; Sayed, A.; Ali, M.; Rahman, G.M.A. Evaluation of ground water resources in Mymensingh Sadar Upazilla, Bangladesh. *Asian J. Agric. Ext. Econ. Soc.* **2015**, *7*, 1–10. [[CrossRef](#)]
5. Fildes, S.G.; Clark, I.F.; Somaratne, N.M.; Ashman, G. Mapping groundwater potential zones using remote sensing and geographical information systems in a fractured rock setting, Southern Flinders Ranges, South Australia. *J. Earth Syst. Sci.* **2020**, *129*, 1–25. [[CrossRef](#)]
6. Hasan, M.R.; Mostafa, M.G.; Rahman, N.; Islam, M.S.; Islam, M.M. Groundwater depletion and its sustainable management in barind tract of Bangladesh. *Res. J. Environ. Sci.* **2018**, *12*, 247–255.
7. Mojid, M.A.; Parvez, M.F.; Mainuddin, M.; Hodgson, G. Water table trend—A sustainability status of groundwater development in North-West Bangladesh. *Water* **2019**, *11*, 1182. [[CrossRef](#)]
8. Rahman, M.; Mahbub, A. Groundwater Depletion with Expansion of Irrigation in Barind Tract: A Case Study of Tanore Upazila. *J. Water Resour. Prot.* **2012**, *4*, 567–575. [[CrossRef](#)]
9. Ahammed, S.; Chung, E.-S.; Shahid, S. Parametric assessment of pre-monsoon agricultural water scarcity in Bangladesh. *Sustainability* **2018**, *10*, 819. [[CrossRef](#)]
10. Yin, S.; Xiao, Y.; Han, P.; Hao, Q.; Gu, X.; Men, B.; Huang, L. Investigation of groundwater contamination and health implications in a typical Semiarid Basin of North China. *Water* **2020**, *12*, 1137. [[CrossRef](#)]
11. Islam, B.; Firoz, A.B.M.; Foglia, L.; Marandi, A.; Khan, A.R.; Schüth, C.; Ribbe, L. A regional groundwater-flow model for sustainable groundwater-resource management in the south Asian megacity of Dhaka, Bangladesh. *Hydrogeol. J.* **2017**, *25*, 617–637. [[CrossRef](#)]
12. Akhter, S.; Sharmin, A.; Islam, T.; Ullah, M. Climatic variability on groundwater recharge of Mymensingh district in Bangladesh. *Progress. Agric.* **2019**, *30*, 104–112. [[CrossRef](#)]
13. Mardy, T.; Uddin, M.N.; Sarker, A.; Roy, D.; Dunn, E.S. Assessing coping strategies in response to drought: A micro level study in the North-West region of Bangladesh. *Climate* **2018**, *6*, 23. [[CrossRef](#)]
14. Pourghasemi, H.R.; Beheshtirad, M. Assessment of a data-driven evidential belief function model and GIS for groundwater potential mapping in the Koohrang Watershed, Iran. *Geocarto Int.* **2015**, *30*, 662–685. [[CrossRef](#)]
15. Chowdhury, A.; Jha, M.K.; Chowdary, V.M.; Mal, B.C. Integrated remote sensing and GIS-based approach for assessing groundwater potential in West Medinipur district, West Bengal, India. *Int. J. Remote Sens.* **2009**, *30*, 231–250. [[CrossRef](#)]
16. Ozdemir, A. GIS-based groundwater spring potential mapping in the Sultan Mountains (Konya, Turkey) using frequency ratio, weights of evidence and logistic regression methods and their comparison. *J. Hydrol.* **2011**, *411*, 290–308. [[CrossRef](#)]
17. Lee, S.; Kim, Y.S.; Oh, H.J. Application of a weights-of-evidence method and GIS to regional groundwater productivity potential mapping. *J. Environ. Manag.* **2012**, *96*, 91–105. [[CrossRef](#)] [[PubMed](#)]

18. Chenini, I.; Mammou, A.B. Groundwater recharge study in arid region: An approach using GIS techniques and numerical modeling. *Comput. Geosci.* **2010**, *36*, 801–817. [[CrossRef](#)]
19. Razandi, Y.; Pourghasemi, H.R.; Neisani, N.S.; Rahmati, O. Application of analytical hierarchy process, frequency ratio, and certainty factor models for groundwater potential mapping using GIS. *Earth Sci. Inform.* **2015**, *8*, 867–883. [[CrossRef](#)]
20. Naghibi, S.A.; Pourghasemi, H.R.; Pourtaghi, Z.S.; Rezaei, A. Groundwater qanat potential mapping using frequency ratio and Shannon's entropy models in the Moghan watershed, Iran. *Earth Sci. Inform.* **2015**, *8*, 171–186. [[CrossRef](#)]
21. Rahmati, O.; Pourghasemi, H.R.; Melesse, A.M. Application of GIS-based data driven random forest and maximum entropy models for groundwater potential mapping: A case study at Mehran Region, Iran. *CATENA* **2016**, *137*, 360–372. [[CrossRef](#)]
22. Shamsudduha, M.; Joseph, G.; Haque, S.S.; Khan, M.R.; Zahid, A.; Ahmed, K.M.U. Multi-hazard groundwater risks to water supply from shallow depths: Challenges to achieving the sustainable development goals in Bangladesh. *Expos. Health* **2020**, *12*, 657–670. [[CrossRef](#)]
23. Saranya, T.; Saravanan, S. Groundwater potential zone mapping using analytical hierarchy process (AHP) and GIS for Kancheepuram District, Tamilnadu, India. *Model. Earth Syst. Environ.* **2020**, *6*, 1105–1122. [[CrossRef](#)]
24. Forkuor, G.; Pavelic, P.; Asare, E.; Obuobie, E. Modelling potential areas of groundwater development for agriculture in northern Ghana using GIS/RS. *Hydrol. Sci. J.* **2013**, *58*, 437–451. [[CrossRef](#)]
25. Luo, D.; Wen, X.; Zhang, H.; Xu, J.; Zhang, R. An improved FAHP based methodology for groundwater potential zones in Longchuan River basin, Yunnan Province, China. *Earth Sci. Inform.* **2020**, *13*, 847–857. [[CrossRef](#)]
26. Allafta, H.; Opp, C.; Patra, S. Identification of groundwater potential zones using remote sensing and GIS techniques: A case study of the Shatt Al-Arab Basin. *Remote Sens.* **2021**, *13*, 112. [[CrossRef](#)]
27. Reddy, Y.V.K.; Lakshmi, S.V. Identification of groundwater potential zones using GIS and remote sensing. *Water* **2018**, *119*, 3195–3210.
28. Abuzied, S.M.; Alrefae, H.A. Mapping of groundwater prospective zones integrating remote sensing, geographic information systems and geophysical techniques in El-Qaà Plain area, Egypt. *Hydrogeol. J.* **2017**, *25*, 2067–2088. [[CrossRef](#)]
29. Machiwal, D.; Jha, M.K.; Mal, B.C. Assessment of groundwater potential in a semi-arid region of india using remote sensing, GIS and MCDM techniques. *Water Resour. Manag.* **2010**, *25*, 1359–1386. [[CrossRef](#)]
30. Ahirwar, S.; Malik, M.S.; Ahirwar, R.; Shukla, J.P. Application of remote sensing and GIS for groundwater recharge potential zone mapping in upper betwa watershed. *J. Geol. Soc. India* **2020**, *95*, 308–314. [[CrossRef](#)]
31. Jhariya, D.C.; Kumar, T.; Gobinath, M.; Diwan, P.; Kishore, N. Assessment of groundwater potential zone using remote sensing, GIS and multi criteria decision analysis techniques. *J. Geol. Soc. India* **2016**, *88*, 481–492. [[CrossRef](#)]
32. Andualem, T.G.; Demeke, G.G. Groundwater potential assessment using GIS and remote sensing: A case study of Guna tana landscape, upper blue Nile Basin, Ethiopia. *J. Hydrol. Reg. Stud.* **2019**, *24*, 100610. [[CrossRef](#)]
33. Fashae, O.A.; Tijani, M.N.; Talabi, A.O.; Adedeji, O.I. Delineation of groundwater potential zones in the crystalline basement terrain of SW-Nigeria: An integrated GIS and remote sensing approach. *Appl. Water Sci.* **2013**, *4*, 19–38. [[CrossRef](#)]
34. Agarwal, E.; Agarwal, R.; Garg, R.D.; Garg, P.K. Delineation of groundwater potential zone: An AHP/ANP approach. *J. Earth Syst. Sci.* **2013**, *122*, 887–898. [[CrossRef](#)]
35. Bera, A.; Mukhopadhyay, B.P.; Barua, S. Delineation of groundwater potential zones in Karha river basin, Maharashtra, India, using AHP and geospatial techniques. *Arab. J. Geosci.* **2020**, *13*, 693. [[CrossRef](#)]
36. Agarwal, R.; Garg, P.K. Remote sensing and GIS based groundwater potential & recharge zones mapping using multi-criteria decision-making technique. *Water Resour. Manag.* **2016**, *30*, 243–260. [[CrossRef](#)]
37. Bangladesh Bureau of Statistics (BBS). *Population Census-2011. Preliminary Report. Bangladesh Bureau of Statistics 2011*; Ministry of Planning: Dhaka, Bangladesh, 2011.
38. Pradhan, N.; Das, P.; Gupta, N.; Shrestha, A. Sustainable management options for healthy rivers in South Asia: The case of Brahmaputra. *Sustainability* **2021**, *13*, 1087. [[CrossRef](#)]
39. Akter, S.; Ali, R.M.E.; Karim, S.; Khatun, M.; Alam, M.F. Geomorphological, geological and engineering geological aspects for sustainable urban planning of Mymensingh City, Bangladesh. *Open J. Geol.* **2018**, *8*, 737–752. [[CrossRef](#)]
40. Afrin, N.; Habiba, U.; Das, R.; Auyon, S.T.; Islam, M. Impact and vulnerability assessment on climate change of Jessore and Mymensingh districts in Bangladesh. *Progress. Agric.* **2018**, *29*, 320–335.
41. Chakraborty, D.; Khatun, M.M.; Alam, I. Rainfall in Bangladesh. *J. Eng. Res. Rep.* **2021**, 103–112. [[CrossRef](#)]
42. Bangladesh Bureau of Statistics (BBS); Ministry of Planning. *Bangladesh Population and Housing Census 2011, District Report: Mymensingh*; Government of the People's Republic of Bangladesh: Dhaka, Bangladesh, 2015; ISBN 978-948-33-8614-4.
43. Hussain, M.; Bari, S.H.; Tarif, M.E.; Rahman, T.U.; Hoque, M.A. Temporal and spatial variation of groundwater level in Mymensingh district, Bangladesh. *Int. J. Hydrol. Sci. Technol.* **2016**, *6*, 188. [[CrossRef](#)]
44. Rwanga, S.S.; Ndambuki, J.M. Accuracy assessment of land use/land cover classification using remote sensing and GIS. *Int. J. Geosci.* **2017**, *8*, 611–622. [[CrossRef](#)]
45. Owolabi, S.T.; Madi, K.; Kalumba, A.M.; Orimoloye, I.R. A groundwater potential zone mapping approach for semi-arid environments using remote sensing (RS), geographic information system (GIS), and analytical hierarchical process (AHP) techniques: A case study of Buffalo catchment, Eastern Cape, South Africa. *Arab. J. Geosci.* **2020**, *13*, 1184. [[CrossRef](#)]
46. Saaty, T.L. Decision making with the analytic hierarchy process. *Int. J. Serv. Sci.* **2008**, *1*, 83–98. [[CrossRef](#)]

47. Das, B.; Pal, S.C.; Malik, S.; Chakraborty, R. Modeling groundwater potential zones of Puruliya district, West Bengal, India using remote sensing and GIS techniques. *Geol. Ecol. Landsc.* **2018**, *3*, 223–237. [[CrossRef](#)]
48. Atmaja, R.R.S.; Putra, D.P.E.; Setijadji, L.D. Delineation of groundwater potential zones using remote sensing, GIS, and AHP techniques in southern region of Banjarnegara, Central Java, Indonesia. In Proceedings of the Sixth Geoinformation Science Symposium, Yogyakarta, Indonesia, 26–27 August 2019; p. 11311. [[CrossRef](#)]
49. Tolche, A.D. Groundwater potential mapping using geospatial techniques: A case study of Dhungeta-Ramis sub-basin, Ethiopia. *Geol. Ecol. Landsc.* **2020**, *5*, 65–80. [[CrossRef](#)]
50. Saaty, T. *The Analytic Hierarchy Process*; McGraw-Hill: New York, NY, USA, 1980.
51. Saaty, T.L. How to make a decision: The analytic hierarchy process. *Eur. J. Operat. Res.* **1990**, *48*, 9–26. [[CrossRef](#)]
52. Nowreen, S.; Newton, I.H.; Zzaman, R.U.; Islam, A.K.M.S.; Islam, G.M.T.; Alam, S. Development of potential map for groundwater abstraction in the northwest region of Bangladesh using RS-GIS-based weighted overlay analysis and water-table-fluctuation technique. *Environ. Monit. Assess.* **2021**, *193*, 24. [[CrossRef](#)]
53. Basavarajappa, H.T.; Dinakar, S.; Manjunatha, M.C. Validation of derived groundwater potential zones (gwpz) using geoinformatics and actual yield from well points in parts of upper cauvery basin of mysuru and chamarajanagara districts, karntaka, India. *Int. J. Civil Eng. Technol.* **2016**, *7*, 141–161.
54. Jensen, J.R. *Introductory Digital Image Processing: A Remote Sensing Perspective*, 2nd ed.; Prentice Hall Inc.: Upper Saddle River, NJ, USA, 1996.
55. Raju, R.S.; Raju, G.S.; Rajasekhar, M. Identification of groundwater potential zones in Mandavi River basin, Andhra Pradesh, India using remote sensing, GIS and MIF techniques. *HydroResearch* **2019**, *2*, 1–11. [[CrossRef](#)]
56. Usman, M.; Liedl, R.; Shahid, M.A.; Abbas, A. Land use/land cover classification and its change detection using multi-temporal MODIS NDVI data. *J. Geogr. Sci.* **2015**, *25*, 1479–1506. [[CrossRef](#)]
57. Tam, V.T.; De Smedt, F.; Batelaan, O.; Dassargues, A.; Smedt, F. Study on the relationship between lineaments and borehole specific capacity in a fractured and karstified limestone area in Vietnam. *Hydrogeol. J.* **2004**, *12*, 662–673. [[CrossRef](#)]
58. Todd, D.K.; Mays, L.W. *Groundwater Hydrology*, 3rd ed.; John Wiley & Sons: Hoboken, NJ, USA, 2013.
59. Castillo, J.L.U.; Leal, J.A.R.; Cruz, D.A.M.; Martínez, A.C.; Celestino, A.E.M. Identification of the dominant factors in groundwater recharge process, using multivariate statistical approaches in a semi-arid region. *Sustainability* **2021**, *13*, 11543. [[CrossRef](#)]
60. Masoud, A.M.; Pham, Q.B.; Alezabawy, A.K.; Abu El-Magd, S.A. Efficiency of geospatial technology and multi-criteria decision analysis for groundwater potential mapping in a semi-arid region. *Water* **2022**, *14*, 882. [[CrossRef](#)]
61. Ahmed, R.; Sajjad, H. Analyzing factors of groundwater potential and its relationship with population in the Lower Barpani Watershed, Assam, India. *Nat. Resour. Res.* **2018**, *27*, 503–515. [[CrossRef](#)]
62. Rajaveni, S.P.; Brindha, K.; Elango, L. Geological and geomorphological controls on groundwater occurrence in a hard rock region. *Appl. Water Sci.* **2017**, *7*, 1377–1389. [[CrossRef](#)]
63. Lee, B.; Hamm, S.-Y.; Jang, S.; Cheong, J.-Y.; Kim, G.-B. Relationship between groundwater and climate change in South Korea. *Geosci. J.* **2013**, *18*, 209–218. [[CrossRef](#)]
64. Kumar, V.A.; Mondal, N.C.; Ahmed, S. Identification of groundwater potential zones using RS, GIS and AHP techniques: A case study in a part of Deccan Volcanic Province (DVP), Maharashtra, India. *J. Indian Soc. Remote Sens.* **2020**, *48*, 497–511. [[CrossRef](#)]
65. Landis, J.R.; Koch, G.G. A one-way components of variance model for categorical data. *Biometrics* **1977**, *33*, 671–679. [[CrossRef](#)]
66. Inglezakis, V.; Pouloupoulos, S.; Arkhangelsky, E.; Zorpas, A.; Menegaki, A. Chapter 3—Aquatic environment. In *Environment and Development*; Stavros, G., Pouloupoulos, S.G., Vassilis, J.I., Eds.; Elsevier: Amsterdam, The Netherlands, 2016; pp. 137–212. [[CrossRef](#)]
67. Salam, M.A.; Kabir, M.M.; Yee, L.F.; Rak, A.A.E.; Khan, M.S. Water quality assessment of Perak River, Malaysia. *Pollution* **2019**, *5*, 637–648. [[CrossRef](#)]
68. Hasan, F.; Alam, N.E.; Salam, M.; Rahman, H.; Paul, S.; Rak, A.; Ambade, B.; Islam, A.T. Health risk and water quality assessment of surface water in an urban river of Bangladesh. *Sustainability* **2021**, *13*, 6832. [[CrossRef](#)]
69. Salam, M.A.; Paul, S.C.; Zain, R.A.M.M.; Bhowmik, S.; Nath, M.R.; Siddiqua, S.A.; Das Aka, T.; Iqbal, M.A.; Kadir, W.R.; Ahamad, R.B.; et al. Trace metals contamination potential and health risk assessment of commonly consumed fish of Perak River, Malaysia. *PLoS ONE* **2020**, *15*, e0241320. [[CrossRef](#)] [[PubMed](#)]
70. Wada, Y.; Van Beek, L.P.H.; Van Kempen, C.M.; Reckman, J.W.T.M.; Vasak, S.; Bierkens, M.F.P. Global depletion of groundwater resources. *Geophys. Res. Lett.* **2010**, *37*, L20402. [[CrossRef](#)]
71. Guerrero-Morales, J.; Fonseca, C.; Gómez-Albores, M.; Sampedro-Rosas, M.; Silva-Gómez, S. Proportional variation of potential groundwater recharge as a result of climate change and land-use: A study case in Mexico. *Land* **2020**, *9*, 364. [[CrossRef](#)]
72. Karlović, I.; Marković, T.; Vujnović, T. Groundwater recharge assessment using multi component analysis: Case study at the NW edge of the Varaždin Alluvial Aquifer, Croatia. *Water* **2022**, *14*, 42. [[CrossRef](#)]
73. Da Costa, A.; De Salis, H.; Viana, J.; Pacheco, F.L. Groundwater recharge potential for sustainable water use in urban areas of the Jequitiba River Basin, Brazil. *Sustainability* **2019**, *11*, 2955. [[CrossRef](#)]
74. Arulbalaji, P.; Padmalal, D.; Sreelash, K. GIS and AHP techniques based delineation of groundwater potential zones: A case study from Southern Western Ghats, India. *Sci. Rep.* **2019**, *9*, 2082. [[CrossRef](#)] [[PubMed](#)]
75. Dar, T.; Rai, N.; Bhat, A. Delineation of potential groundwater recharge zones using analytical hierarchy process (AHP). *Geol. Ecol. Landsc.* **2020**, *5*, 292–307. [[CrossRef](#)]

76. Qureshi, A.S.; Ahmed, J.; Krupnik, T.J. *Groundwater Management in Bangladesh: An Analysis of Problems and Opportunities*; Research Report No. 2; Cereal Systems Initiative for South Asia Mechanization, and Irrigation (CSISA-MI): Dhaka, Bangladesh, 2015. [[CrossRef](#)]
77. Aziz, N.; Nilufar, F. Effects of growth on urban morphology and land use pattern in mymensingh: A historic town of Bangladesh. *Nakhara J. Environ. Des. Plan.* **2019**, *16*, 53–68. [[CrossRef](#)]
78. Ifediegwu, S.I. Assessment of groundwater potential zones using GIS and AHP techniques: A case study of the Lafia district, Nasarawa State, Nigeria. *Appl. Water Sci.* **2022**, *12*, 10. [[CrossRef](#)]
79. Talukdar, S.; Mallick, J.; Sarkar, S.K.; Roy, S.K.; Islam, A.R.M.T.; Praveen, B.; Naikoo, M.W.; Rahman, A.; Sobnam, M. Novel hybrid models to enhance the efficiency of groundwater potentiality model. *Appl. Water Sci.* **2022**, *12*, 62. [[CrossRef](#)]
80. Subramani, T.; Santhi, D. Groundwater potential and recharge zone mapping for Namakkal Town using RS & GIS. *Int. J. Eng. Technol.* **2018**, *7*, 155. [[CrossRef](#)]
81. Jahan, C.S.; Rahaman, F.; Arefin, R.; Ali, S.; Mazumder, Q.H. Delineation of groundwater potential zones of Atrai-Sib River basin in north-west Bangladesh using remote sensing and GIS techniques. *Sustain. Water Resour. Manag.* **2018**, *5*, 689–702. [[CrossRef](#)]
82. Arefin, R. Groundwater potential zone identification using an analytic hierarchy process in Dhaka City, Bangladesh. *Environ. Earth Sci.* **2020**, *79*, 268. [[CrossRef](#)]
83. Rana, M.M.S.P.; Hossain, M.A.; Nasher, N.M.R. Identification of groundwater potential zone using geospatial techniques of agriculture dominated area in Dinajpur district, Bangladesh. *Environ. Chall.* **2022**, *7*, 100475. [[CrossRef](#)]
84. Babu, M.A.H.; Islam, M.R.; Farzana, F.; Uddin, M.J.; Islam, M.S. Application of GIS and remote sensing for identification of groundwater potential zone in the Hilly Terrain of Bangladesh. *Grassroots J. Nat. Resour.* **2020**, *3*, 16–27. [[CrossRef](#)]
85. Ahmed, N.; Hoque, M.A.-A.; Pradhan, B.; Arabameri, A. Spatio-temporal assessment of groundwater potential zone in the drought-prone area of Bangladesh using GIS-based bivariate models. *Nat. Resour. Res.* **2021**, *30*, 3315–3337. [[CrossRef](#)]